On the Performance of IRS-Assisted OFDM System with Non-Ideal Oscillator and Amplifier

Khagendra Joshi, Mohd Hamza Naim Shaikh, Sana Ali Naqvi and Vivek Ashok Bohara

Abstract—Intelligent reflective surface (IRS), a software-controlled metasurface, is now a proven and promising candidate technology to achieve superior and reliable data transmission for the next-generation mobile communication systems. This letter investigates the performance of an IRS-assisted orthogonal frequency division multiplexing (OFDM) wireless system in the presence of a non-ideal oscillator and amplifier. The analytical framework comprises of deriving the closed-form expressions for the outage probability (OP), spectral efficiency (SE), energy efficiency (EE), and diversity order. The result shows that the phase noise and distortion significantly limit the performance gain of an IRS-assisted OFDM wireless communication system.

Keywords— Performance analysis, OFDM, spectral efficiency, intelligent reflecting surface, outage, phase noise, nonlinearity, energy efficiency

I. INTRODUCTION

Various technologies like massive multiple-input multiple-output (MIMO), millimeter-wave (mm-Wave) communication, ultra-dense networks (UDN), etc., have been utilized to cater to the throughput and channel capacity demands for fifth-generation (5G) wireless communication. The 5G cellular standard assures enhanced data rates, better coverage, transmission reliability, and minimum latency. 5G cellular standard, like its predecessor fourth-generation (4G), incorporates the orthogonal frequency division multiplexing (OFDM) and its variants as the preferred modulation scheme [1]. However, OFDM is highly sensitive to frequency synchronization, causing phase noise in the presence of non-ideal oscillators. Further, the high peak-to-average-power ratio (PAPR) of OFDM also causes nonlinear distortions in the high power amplifiers (HPA) [2]. The theoretical analysis of nonlinear distortions in OFDM signals is investigated in [2].

Intelligent reflecting surface (IRS) is a revolutionary technology that assists the implementation of ultra-broadband connectivity for the futuristic 6G wireless system [3]. IRS consists of a planar surface comprised of a large number of passive reflecting unit cells (RUs), wherein each of these elements can independently alter the phase and/or attenuation of the incident signal. By densely deploying these IRSs in the wireless network and controlling the reflection of each unit cell, the signal transmission between transmitters and receivers can be easily reconfigured to enhance received signal strength. Thus, by regulating the wireless propagation environment, IRS can provide high energy efficiency (EE) and spectral efficiency (SE) [4].
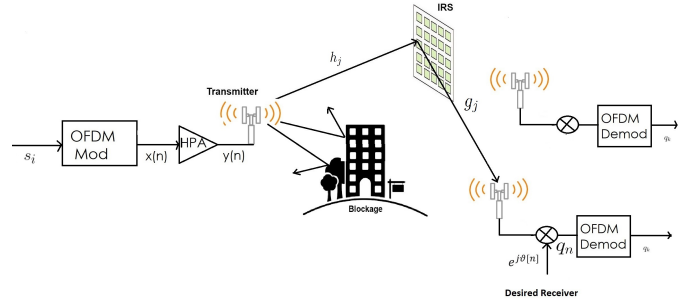
Fig. 1: Schematic for the IRS-assisted OFDM wireless system

The performance of an IRS-assisted wireless network has been analyzed in several works like [5]–[8] and the references within. Specifically, [5] measures the system performance based upon the outage probability, where the channels associated with IRS are LoS, and the phase error for each unit cell follows a von mises distribution. Likewise, [6] investigates the outage performance with statistical channel state information (CSI) over Rician fading channels. All these prior works assume the presence of ideal transceivers. However, in practice, hardware imperfections are causing in-phase and quadrature imbalance, nonlinear distortion, and phase noise. Further, this phase noise causes common phase error (CPE) and inter-carrier interference (ICI). These imperfections can significantly limit the performance of IRS-assisted wireless systems [9], [10].

As evident, the existing research in IRS focuses mainly on the frequency-flat channels [9], [10]. Recently, a merger of OFDM and IRS have been proposed in [11]. Taking motivation from the above, we investigate an IRS-assisted OFDM system with frequency-selective channels in the presence of practical oscillators and amplifiers. Distinctively, in the proposed work, we evaluate the performance of an IRS-assisted non-ideal transceiver-based OFDM system in terms of the outage probability (OP), SE, and EE. Simulation results further verify the exactness of the derived analytical expressions.

II. SYSTEM MODEL

Fig. 1 represents the system model of an OFDM-based IRS-assisted wireless communication system. In the absence of a direct link between the transmitter (Tx) and receiver (Rx), an IRS with M reflecting unit cells (RUs) is facilitating the transmission. The channel between the Tx and the j-th RU is denoted by h_j, while the channel between the j-th RU and the Rx is g_j. Similar to [9], both the channels are assumed to be

independent and identically distributed (i.i.d) and characterized by the Rayleigh fading model.

In general, the complex baseband characterization of an OFDM signal with N subcarriers is represented by

$$x(n) = \frac{1}{N} \sum_{i=0}^{N-1} s_i e^{\frac{j2\pi in}{N}}, \tag{1}$$

where i denotes the subcarrier index, s_i are the complex data symbols, and n represents the discrete time domain sample. Without loss of generality, we consider that s_i are i.i.d random variables with zero mean and variance P_t. According to the central limit theorem, for large N, the $x(n)$ can be considered as a complex Gaussian process with a zero mean and variance $P_{av} = \frac{P_t}{N}$ [12].

A. Transceiver Impairments

Further, a practical transceiver architecture always suffers from unavoidable additive distortions such as I/Q imbalance, radio frequency (RF) nonlinearity of the high power amplifier (HPA), and phase noise due to non-ideal oscillators. Due to these hardware impairments, there is a mismatch between the desired and the actual transmitted OFDM signal. Here, we briefly explain the nonlinearity and the phase noise model.

HPA Model: The nonlinear representation of the HPA can be designed by the baseband polynomial model and it can be expressed as

$$y(n) = \sum_{k=1}^{K} \alpha_k x(n) |x(n)|^{k-1}, \tag{2}$$

where $y(n)$ and $x(n)$ are the output and input signal of the HPA respectively, α_k are the complex nonlinear coefficients, and K is the order of non-linearity. As the odd order components (mainly IM3 and IM5) generate the most in-band distortion, our prime consideration is the odd order nonlinearity. As a good resemblance, we limit the non-linearity order to the third degree [12], which can be expressed as

$$y(n) = \alpha_1 x(n) + \alpha_3 x(n) |x(n)|^2. \tag{3}$$

The resultant output signal of the HPA can be represented as

$$y(n) = \mu x(n) + \xi(n), \tag{4}$$

where μ is the complex attenuation factor and $\xi(n)$ is the additive Gaussian noise due to the distortion in the HPA. The detailed characterization of μ and $\xi(n)$ can be found in [12]. Hence, for the sake of brevity, it is omitted here.

Phase Noise Model: Similar to [2], this work models the phase noise as an i.i.d. Gaussian random variable $\vartheta(t) \sim \mathcal{N}\left(0, \sigma_\vartheta^2\right)$. The variance of phase noise, σ_ϑ^2, depends on the oscillator parameters as

$$\sigma_\vartheta^2 = \frac{2K_\vartheta}{\pi} \tan^{-1}\left(\frac{B}{B_{3\text{dB}}}\right) + \frac{BN_f}{\pi}, \tag{5}$$

where $B_{3\text{dB}}$ is the half-power bandwidth, K_ϑ is the phase noise factor, N_f is the noise floor, and B is the signal bandwidth.

Received Signal: Here, we characterize the received signal impaired by non-linear HPA and the phase noise introduced at the receiver due to non-ideal oscillators. After down conversion, the baseband received OFDM symbol from the j-th RU can be expressed as

$$q(n) = [h_j g_j r_j (\mu x(n) + \xi(n)) + n_o(k)] e^{\vartheta(n)}, \tag{6}$$

Here, r_j denotes the response of the j-th RU. The IRS is always configured to provide optimal phase shifts at all the RUs, thus, utilizing (19-20) of [10], and after taking DFT of the signal at the receiver, we get

$$q_i = \frac{1}{N} \sum_{i'=0}^{N-1} \left[\mathcal{H}\left(\mu s_{i'} + \xi(i')\right) + n_o(i') \right] e^{\vartheta(n)} e^{\frac{-j2\pi(i'-i)n}{N}}, \tag{7}$$

where, $\mathcal{H} = \sum_{j=1}^{M} |h_j| |g_j|$.

The characterization for $\mathcal{H}$ can be found in [13], which shows that the probability density function (PDF) and cumulative distribution function (CDF) of $\mathcal{H}$ can be given as

$$f_{\mathcal{H}}(x) = \frac{x^a}{b^{a+1}\Gamma(a+1)} \exp\left(-\frac{x}{b}\right), \tag{8}$$

and

$$F_{\mathcal{H}}(x) = \frac{\gamma\left(1+a, \frac{x}{b}\right)}{\Gamma(a+1)}, \tag{9}$$

where, $\gamma(\cdot, \cdot)$ is the lower incomplete Gamma function and $\Gamma(\cdot)$ is the Gamma function. Further, $a = \frac{z_1^2}{z_2} - 1$, $b = \frac{z_2}{z_1}$ with $z_1 = \frac{M\pi}{2}$ and $z_2 = 4M\left(1 - \frac{\pi^2}{16}\right)$.

From here, we can express the received signal as

$$q_i = \sum_{i'=0}^{N-1} \left[\mathcal{H}\left(\mu s_{i'} + \xi\left(i'\right)\right) + n_o\left(i'\right) \right] \zeta(i' - i), \tag{10}$$

which can further be expanded as

$$q_i = \mu \mathcal{H} s_i \zeta(0) + \sum_{i'=0, i' \neq i}^{N-1} \mu \mathcal{H} s_{i'} \zeta\left(i' - i\right)$$
$$+ \sum_{i'=0}^{N-1} \left[\mathcal{H}\xi\left(i'\right) + n_o\left(i'\right) \right] \zeta\left(i' - i\right), \tag{11}$$

where $\zeta(i) = \frac{1}{N} \sum_{i'=0}^{N-1} e^{\vartheta(n)} e^{\frac{j2\pi in}{N}}$, and $\zeta(0)$ denotes the CPE. Further, $\zeta\left(i' - i\right)$ acts as orthogonality breaker of the subcarriers and causes ICI.

The final decoded complex OFDM symbol can be represented as

$$\hat{q}_i = \mu \mathcal{H} s_i \zeta(0) + \sum_{i'=0, i' \neq i}^{N-1} \mu \mathcal{H} s_{i'} \zeta\left(i' - i\right)$$
$$+ \sum_{i'=0}^{N-1} \mathcal{H}\xi\left(i'\right) \zeta\left(i' - i\right) + \hat{n}_i, \tag{12}$$

where, $\hat{n}_i = \sum_{i'=0}^{N-1} n_o \left(i'\right) \zeta \left(i' - i\right)$. or equivalently,

$$\hat{q}_i = \underbrace{\mathcal{H} \, \mu s_i \zeta(0)}_{Signal\ with\ CPE} + \underbrace{\mathcal{H}\mu \sum_{i'=0, i'\neq i}^{N-1} s_{i'} \zeta \left(i' - i\right)}_{ICI\ Signal}$$

$$+ \underbrace{\mathcal{H} \sum_{i'=0}^{N-1} \xi \left(i'\right) \zeta \left(i' - i\right)}_{nonlinear\ distortion} + \underbrace{\hat{n}_i}_{AWGN}. \quad (13)$$

III. PERFORMANCE ANALYSIS

Initially, we derive the signal-to-distortion-plus-interference-noise ratio (SDINR), which is then utilized for evaluating the OP, SE and EE. The SDINR for the proposed IRS-assisted OFDM system can be evaluated as

$$SDINR = \frac{P_{cpe}\mathcal{H}^2/P_t}{\mathcal{H}^2(P_{ici} + P_{nd})/P_t + 1/\rho_t}, \quad (14)$$

where, P_{cpe} is the power of the required signal affected with CPE and an attenuation factor. $\mathcal{H}$ is the equivalent transmitter-IRS-receiver channel gain. P_{ici} is the the variance of ICI. P_{nd} is the variance of the nonlinear distortion noise, respectively. Further, $\rho_t = P_t/P_n$, indicates the transmit signal-to-noise ratio (SNR).

Hence, the average power of the required signal with an attenuation factor can be defined as follows

$$P_{cpe} = \text{Var}[\mu s_i \zeta(0)],$$
$$= \mu^2 \text{Var}[s_i \zeta(0)]. \quad (15)$$

Utilizing variance properties and (54-58) of [2], we get

$$P_{cpe} = \mu^2 P_t \left\{ \frac{1 - e^{-\sigma_\vartheta^2}}{N} + e^{-\sigma_\vartheta^2} \right\}. \quad (16)$$

The variance of the ICI can be expressed as

$$P_{ici} = \mu^2 \text{Var} \left[\sum_{i'=0|i'\neq i}^{N-1} s_{i'} \zeta(i' - i) \right], \quad (17)$$

which after some manipulation and substitutions can be given as

$$P_{ici} = \mu^2 P_t \left(1 - \frac{1}{N}\right) \left(1 - e^{-\sigma_\vartheta^2}\right). \quad (18)$$

Further, the variance of non-linear distortion can be given as

$$P_{nd} = \sum_{i'=0}^{N-1} \text{Var}[\xi(i')\zeta(i' - i)]. \quad (19)$$

Using (54-58) of [2], we get

$$P_{nd} = \sigma_\xi^2$$
$$= |\alpha_3|^2 P_t^3 \frac{3N^2 - 11N + 12}{N^4}. \quad (20)$$

A. Outage Probability

The OP for the IRS-assisted OFDM system, P_{op}, can be written in terms of the rate threshold, R_{th}, as

$$P_{op} = \text{Pr}\left[\log_2\left(1 + SDINR\right) < R_{th}\right]. \quad (21)$$

Utilizing (14), P_{op} can be evaluated as

$$P_{op} = \text{Pr}\left[\log_2\left(1 + \frac{P_{cpe}\mathcal{H}^2/P_t}{\mathcal{H}^2(P_{ici} + P_{nd})/P_t + \frac{1}{\rho_t}}\right) < R_{th}\right],$$
$$= \text{Pr}\left[\frac{P_{cpe}\mathcal{H}^2/P_t}{\mathcal{H}^2(P_{ici} + P_{nd})/P_t + \frac{1}{\rho_t}} < \rho_{th}\right],$$
$$= \text{Pr}\left[\mathcal{H} < \Omega\right], \quad (22)$$

where $\Omega^{-1} = \sqrt{\frac{P_{cpe}\rho_t}{P_t\rho_{th}} - \frac{(P_{ici}+P_{nd})\rho_t}{P_t}}$ and $\rho_{th} = 2^{R_{th}} - 1$. After simplifying the above equation, the OP of the considered system, P_{op}, can be evaluated as

$$P_{op} = \int_0^\Omega f_{\mathcal{H}}(x)dx$$
$$= \frac{\gamma\left(a + 1, \Omega/b\right)}{\Gamma\left(a + 1\right)}. \quad (23)$$

B. Spectral Efficiency

Likewise, the SE can be defined as

$$SE = \int_0^\infty \log_2\left(1 + SDINR\right) f_{\mathcal{H}}(x)\text{dx}, \quad (24)$$

which on utilizing the distribution of $\mathcal{H}$ gives

$$SE = \int_0^\infty \log_2\left(1 + \frac{P_{cpe}x^2/P_t}{x^2(P_{ici} + P_{nd})/P_t + \frac{1}{\rho_t}}\right) f_{\mathcal{H}}(x)\text{dx}, \quad (25)$$

Utilizing (8), it can be re-written as

$$SE = \frac{1}{b^{a+1}\Gamma(a + 1)\ln 2} \times$$
$$\int_0^\infty \ln\left(1 + \frac{P_{cpe}\mathcal{H}^2/P_t}{\mathcal{H}^2(P_{ici} + P_{nd})/P_t + \frac{1}{\rho_t}}\right) x^a e^{\left(-\frac{x}{b}\right)}\text{dx}. \quad (26)$$

Utilizing [13, eqn 44] for simplifying the above equations, the closed-form solution for the SE can be expressed as (27) shown on the top of the next page[1].

1) *Large M:* For an exceptional instance when the number of reflective unit cells in the IRS is very high, i.e., $M \gg 1$, from (25), the value of x^2 will become larger with increase in the value of M. Thus for large value of M, $(P_{ici} + P_{nd})x^2 \gg 1/\rho_t$. So, in (25), $1/\rho_t$ can be neglected. Thus, after some mathematical simplification, the SE for a larger value of M can be expressed as

$$SE = \log_2\left\{1 + \frac{P_{cpe}}{(P_{ici} + P_{nd})}\right\}. \quad (28)$$

[1]Here $\Upsilon_1 = (P_{cpe} + P_{ici} + P_{nd})\rho_t$ and $\Upsilon_2 = (P_{ici} + P_{nd})\rho_t$.

$$SE = \frac{(a-1)\,\Gamma(a)}{\ln(2)\,\Gamma(a+1)} \left\{ \Upsilon_1 \ln\left(b^2\,\Upsilon_1\right) - \Upsilon_2 \ln\left(b^2\,\Upsilon_1\right) \right\}$$
$$+ \frac{\pi\,\csc\left(a\pi/2\right)}{(2+a)\,b^{a+2}\,\Gamma(a+1)} \left\{ \frac{1}{(\Upsilon_2)^{\frac{a}{2}+1}} \,_1F_2\left(1+\frac{a}{2};\frac{3}{2},2+\frac{a}{2},\frac{-1}{4\,b^2\,\Upsilon_2}\right) - \frac{1}{(\Upsilon_1)^{\frac{a}{2}+1}} \,_1F_2\left(1+\frac{a}{2};\frac{3}{2},2+\frac{a}{2},\frac{-1}{4\,b^2\,\Upsilon_1}\right) \right\}$$
$$+ \frac{\pi\,\sec\left(a\pi/2\right)}{(a+1)\,b^{a+1}\,\Gamma(a+1)} \left\{ \frac{1}{(\Upsilon_2)^{\frac{a+1}{2}}} \,_1F_2\left(\frac{a+1}{2};\frac{1}{2},\frac{a+3}{2},\frac{-1}{4\,b^2\,\Upsilon_2}\right) - \frac{1}{(\Upsilon_1)^{\frac{a+1}{2}}} \,_1F_2\left(\frac{a+1}{2};\frac{1}{2},\frac{a+3}{2},\frac{-1}{4\,b^2\,\Upsilon_1}\right) \right\}$$
$$+ \frac{a\,\Gamma(a)}{\Gamma(a+1)} \left\{ \,_2F_3\left(1,1;2,\frac{1-a}{2},\frac{a-3}{2},\frac{-1}{4\,b^2\,\Upsilon_1}\right) - \,_2F_3\left(1,1;2,\frac{1-a}{2},\frac{a-3}{2},\frac{-1}{4\,b^2\,\Upsilon_2}\right) \right\} \tag{27}$$

2) High Transmit SNR: For the exceptional case when ρ_t is very high, i.e., $\rho_t \to \infty$, from (25), after some simplification the SE can be written as

$$\lim_{\rho_t \to \infty} SE = \log_2 \left\{ 1 + \frac{P_{cpe}}{(P_{ici} + P_{nd})} \right\}. \tag{29}$$

From (28) and (29), it can be concluded that the spectral efficiency saturates in both the above cases, i.e., for a large number of RUs and high transmit SNR. Thus, SE can neither be enhanced by increasing the number of RUs nor the transmit SNR.

C. Energy Efficiency

The EE is the ratio of the SE and the total consumed power, and is measured in bits/Joule/Hz

$$EE = \frac{SE}{P_{total}}, \tag{30}$$

where P_{total} represents the total power consumed in circuit as well as transmit power [10].

So, on expanding the total power, the EE of the IRS-assisted OFDM system can be expressed as

$$EE = \frac{SE}{(1+\beta)P_t + P_c^S + MP_{IRS} + P_c^D}, \tag{31}$$

where, P_t is the source transmit power, P_{IRS} is the total power consumed at each RU, and P_c^D is the total consumed power at the receiver circuitry. Further, βP_t denotes the power consumption of HPA while the power consumed by all the other circuit components of the source is represented by P_c^S.

D. Diversity Order

The diversity order of the IRS-assisted wireless network can be analytically evaluated as [13, eqn. 43]

$$D = -\lim_{\rho_t \to \infty} \left(\frac{log_2(P_{op})}{log_2(\rho_t)} \right) \tag{32}$$

After calculating the final value of P_{op} from (23) assuming $\rho_{th} \leqslant \frac{P_{cpe}}{P_{ici}+P_{nd}}$ and putting it in (32), we obtain,

$$D = \frac{M}{2} \frac{\pi^2}{16 - \pi^2} \tag{33}$$

It is clear that the diversity order varies linearly with the number of RUs and is independent of the nonlinearity effects. So as M increases, the performance of the RIS-assisted wireless systems improves significantly.
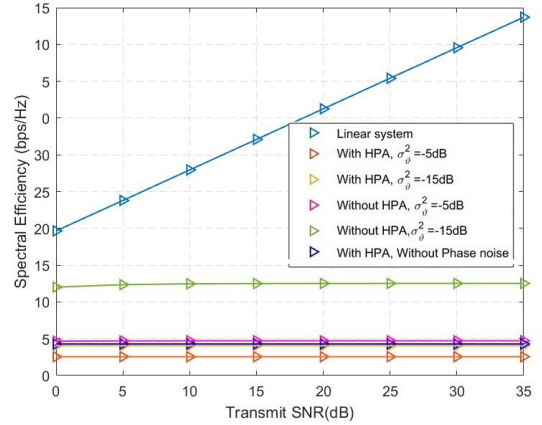
Fig. 2: SE versus transmit SNR (M=10)
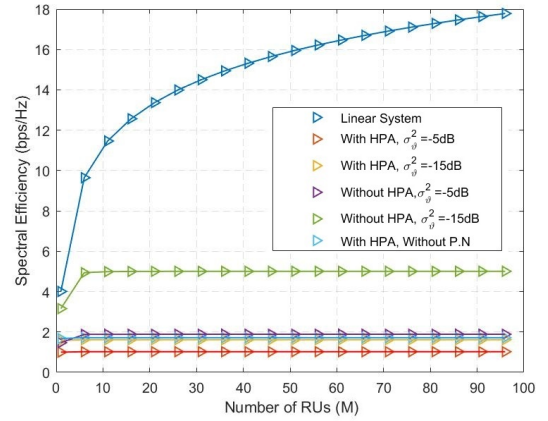
Fig. 3: SE versus M

IV. SIMULATION RESULTS

This part demonstrates the verification of the analytical framework derived in Section III through the OP, SE, and EE simulation results. For the simulation purpose, we have taken N=512, the variance of h_j and $g_j = 1$, $A_{sat} = 5$ volts. Further, P_c^S=10 dBm, P_c^D =10 dBm [3], P_{IRS} = 10 dBm [3], β = 1.25 [10].

Fig. 2 represents the SE with respect to transmit SNR for varying HPA and phase noise variance. It shows how the nonlinear components affect the SE due to the HPA and
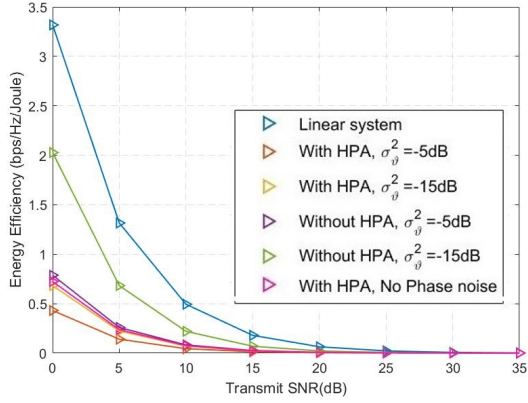
Fig. 4: EE versus transmit SNR (M=10)
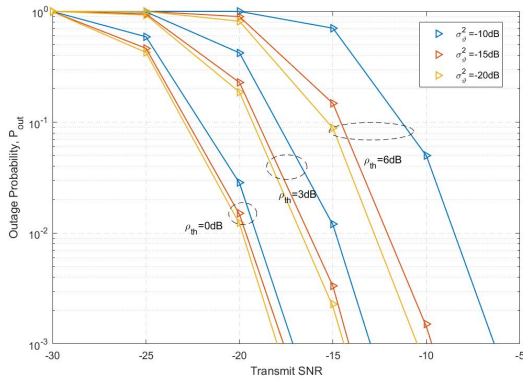
Fig. 5: Analytical (marker points) and simulation (line) results for OP versus transmit SNR (M=10)

phase noise. It can be seen here that the SE saturates with a rise in transmit SNR. This verifies the theoretical expression mentioned in (29). The saturation level depends upon the level of the nonlinear distortion. It can also be noted here that the impact of HPA distortion is more significant than the impact of the phase noise. The system's performance critically degrades due to the presence of non-ideal HPA and a higher value of phase noise.

Fig. 3 represents the plot of SE versus the number of RUs, M, for a fixed value of transmit SNR of 10 dB. The result shows that for an OFDM system, SE saturates with an increase in M for the scenarios with HPA and varying σ_ϑ^2. This can also be inferred analytically from (28).

Fig. 4 represents EE as a function of transmit SNR at $M = 10$, along with the impact of HPA nonlinearity and phase noise. It is clear from the results that the EE reduces with the rise in the value of transmit SNR. Further, the EE improves by reducing the variance of phase noise and distortion due to HPA. It can also be verified that the EE is worse for a system with HPA and $\sigma_\vartheta^2 = -15$ dB. Finally, Fig. 5 represents the plot of OP versus transmit SNR for varying threshold SNR and phase noise variance. The result shows that the outage improves as we reduce the phase noise variance and improves further when the SNR threshold is reduced.

V. CONCLUSION

This work considers an OFDM-based IRS-assisted system with non-ideal oscillators and a high power amplifier. Closed-form expressions of the OP, SE, EE and the diversity order are derived for the considered scenario. The accuracy of this work is verified by comparing the theoretical and simulated results. The results show the significant impact of the nonlinear HPA and phase noise component due to the non-ideal oscillators on the performance of an IRS-assisted OFDM system. The HPA nonlinearity has a more significant impact than the phase noise due to non-ideal oscillators. It can also be observed that at high SNR and for a large number of RUs, SE saturates and cannot be improved further.

REFERENCES

[1] M. Shafi, A. F. Molisch, P. J. Smith, T. Haustein, P. Zhu, P. De Silva, F. Tufvesson, A. Benjebbour, and G. Wunder, "5G: A tutorial overview of standards, trials, challenges, deployment, and practice," *IEEE J. Sel. Areas Commun.*, vol. 35, no. 6, pp. 1201–1221, Jun. 2017.

[2] P. Aggarwal, A. Pradhan, and V. A. Bohara, "A downlink multiuser MIMO-OFDM system with nonideal oscillators and amplifiers: Characterization and performance analysis," *IEEE Systems Journal*, vol. 15, no. 1, pp. 715–726, Mar. 2021.

[3] C. Huang, A. Zappone, G. C. Alexandropoulos, M. Debbah, and C. Yuen, "Reconfigurable intelligent surfaces for energy efficiency in wireless communication," *IEEE Trans. Wireless Commun.*, vol. 18, no. 8, pp. 4157–4170, Aug. 2019.

[4] Q. Wu, S. Zhang, B. Zheng, C. You, and R. Zhang, "Intelligent reflecting surface-aided wireless communications: A tutorial," *IEEE Trans. Commun.*, vol. 69, no. 5, pp. 3313–3351, May 2021.

[5] T. Wang, M.-A. Badiu, G. Chen, and J. P. Coon, "Outage probability analysis of ris-assisted wireless networks with von mises phase errors," *IEEE Wireless Communications Letters*, vol. 10, no. 12, pp. 2737–2741, 2021.

[6] P. Xu, W. Niu, G. Chen, Y. Li, and Y. Li, "Performance analysis of ris-assisted systems with statistical channel state information," *IEEE Transactions on Vehicular Technology*, 2021.

[7] L. Yang, Y. Yang, M. O. Hasna, and M.-S. Alouini, "Coverage, probability of SNR gain, and DOR analysis of RIS-aided communication systems," *IEEE Wireless Commun. Lett.*, vol. 9, no. 8, pp. 1268–1272, Aug. 2020.

[8] Q. Tao, J. Wang, and C. Zhong, "Performance analysis of intelligent reflecting surface aided communication systems," *IEEE Commun. Lett.*, vol. 24, no. 11, pp. 2464–2468, Nov. 2020.

[9] A. A. Boulogeorgos and A. Alexiou, "How much do hardware imperfections affect the performance of reconfigurable intelligent surface-assisted systems?" *IEEE Open J. Commun. Soc.*, vol. 1, pp. 1185–1195, 2020.

[10] M. H. N. Shaikh, V. A. Bohara, A. Srivastava, and G. Ghatak, "Performance analysis of intelligent reflecting surface-assisted wireless system with non-ideal transceiver," *IEEE Open J. Commun. Soc.*, vol. 2, pp. 671–686, 2021.

[11] Y. Yang, B. Zheng, S. Zhang, and R. Zhang, "Intelligent reflecting surface meets OFDM: Protocol design and rate maximization," *IEEE Trans. Commun.*, vol. 68, no. 7, pp. 4522–4535, Jul. 2020.

[12] V. A. Bohara and S. H. Ting, "Theoretical analysis of OFDM signals in nonlinear polynomial models," in *2007 6th Int. Conf. Info., Commun. & Sig. Proces.* IEEE, 2007, pp. 1–5.

[13] A. A. Boulogeorgos and A. Alexiou, "Performance analysis of reconfigurable intelligent surface-assisted wireless systems and comparison with relaying," *IEEE Access*, vol. 8, pp. 94 463–94 483, 2020.